Assembly of Influenza Hemagglutinin Trimers and Its Role in Intracellular Transport

Constance S. Copeland, Robert W. Doms, Eva M. Bolzau, Robert G. Webster,* and Ari Helenius

Department of Cell Biology, Yale University School of Medicine, New Haven, Connecticut 06510; * Department of Virology and Molecular Biology, St. Jude Children's Research Hospital, Memphis, Tennessee 38101.

Abstract. The hemagglutinin (HA) of influenza virus is a homotrimeric integral membrane glycoprotein. It is cotranslationally inserted into the endoplasmic reticulum as a precursor called HA0 and transported to the cell surface via the Golgi complex. We have, in this study, investigated the kinetics and cellular location of the assembly reaction that results in HA0 trimerization. Three independent criteria were used for determining the formation of quaternary structure: the appearance of an epitope recognized by trimer-specific monoclonal antibodies; the acquisition of trypsin resistance, a characteristic of trimers; and the formation of stable complexes which cosedimented with the mature HA0 trimer ($9S_{20,w}$) in sucrose gradients containing Triton X-100.

The results showed that oligomer formation is a posttranslational event, occurring with a half time of ~7.5 min after completion of synthesis. Assembly occurs in the endoplasmic reticulum, followed almost immediately by transport to the Golgi complex. A stabilization event in trimer structure occurs when HA0 leaves the Golgi complex or reaches the plasma membrane. Approximately 10% of the newly synthesized HA0 formed aberrant trimers which were not transported from the endoplasmic reticulum to the Golgi complex or the plasma membrane. Taken together the results suggested that formation of correctly folded quaternary structure constitutes a key event regulating the transport of the protein out of the endoplasmic reticulum. Further changes in subunit interactions occur as the trimers move along the secretory pathway.

Most plasma membrane glycoproteins are comprised of several polypeptide subunits. Assembly of such multi-component proteins into their mature homo- and hetero-oligomeric forms occurs by two general mechanisms. The component polypeptide subunits may be translated together as larger precursors that are then cleaved to give the mature subunit structure. Such proteolytic cleavage steps usually occur relatively late in the secretory pathway. Alternatively, the subunits are synthesized as separate polypeptides and assembled posttranslationally. In this case assembly is thought to occur in the endoplasmic reticulum (ER)[1] or in the Golgi complex (1, 6, 30, 36, 39, 41, 53). Several reports have suggested that subunit assembly is important in the regulation of membrane protein transport in the secretory pathway (6, 10, 28, 41, 42, 55), but little is yet known about the assembly events at the molecular level.

We are studying the properties and intracellular transport of the influenza hemagglutinin (HA), a well characterized viral membrane glycoprotein. HA is a homotrimer, and the subunits (74 kD) consist of two disulfide-bonded glycopolypeptide chains, HA1 and HA2 (see reference 32). The molecule is synthesized and core glycosylated in the ER as a precursor called HA0 which is transported, like cellular plasma membrane proteins, through the Golgi complex to the plasma membrane (37, 46). In passage it undergoes extensive posttranslational modification including trimming of asparagine-linked carbohydrate chains, terminal glycosylation, and fatty acylation (for recent reviews see references 48 and 51). Approximately at the time of insertion into the plasma membrane, the HA0 molecules are cleaved by cellular proteases to yield mature HA (see references 32, 37, and 48). The final subunit structure of mature HA thus arises as a result of both posttranslational assembly and proteolytic cleavage.

The x-ray diffraction structure, available for the trimeric ectodomain of the mature HA, the bromelain fragment of HA (BHA) (66), shows that the three subunits have numerous polar and hydrophobic interactions throughout the 13.5-nm long trimer. Recent work from our lab (15) suggests that hydrophobic interactions between membrane-spanning domains of adjacent subunits also play a role in stabilizing the trimers.

Besides the wealth of structural information, the functions of the hemagglutinin molecule are now reasonably well understood (for reviews see references 23, 32, and 64). The top

1. *Abbreviations used in this paper*: BHA, the bromelain fragment of hemagglutinin comprising the ectodomain of the protein; endo H, endoglycosidase H; ER, endoplasmic reticulum; HA, the cleaved form of hemagglutinin; HA0, the uncleaved precursor of hemagglutinin; TX100, Triton X-100.

domains of the protein spike, consisting of HA1 subunits, attach incoming virus particles to sialic acid residues on the host cell surface. The virus is then taken up by endocytosis and delivered to endosomes, where the low pH triggers an irreversible conformational change in HA which catalyzes fusion between the viral and endosomal membranes. The fusion reaction involves a specific conformational change in the hemagglutinin, which leads to the dissociation of the top domains of the trimeric spike.

Taking advantage of the detailed structural and functional information available on hemagglutinin, we have, in this study, determined the kinetics and the cellular location of trimer assembly. We show that initial interactions between HA0 subunits occur 4–15 min after synthesis. This is just before transfer of HA0 from the ER to the Golgi complex, suggesting that oligomerization may constitute a prerequisite for transport. The complex undergoes a further change upon leaving the Golgi apparatus for the plasma membrane. In addition, few hemagglutinin molecules trimerize into aberrant forms that are not transported from the ER to the Golgi complex. Similar results with the A/Japan/305/57 strain of influenza have recently been obtained by Gething and coworkers using different methods (25).

Materials and Methods

Cells, Vectors, and Virus

CV-1 monkey kidney cells were cultured as described previously (17). The SV-40 late replacement vectors used to express HA0 were kindly provided by Drs. Carolyn Doyle, Joe Sambrook, and Mary-Jane Gething (Department of Biochemistry and Howard Hughes Medical Institute, University of Texas Health Science Center, Dallas, TX). The vectors were SVEXHA (14) for the wild-type X:31 strain of HA and SVEXHA-A$^-$ for the anchor minus form of X:31 HA (18). CV-1 cells were plated (10^6 cells per 90-mm culture dish) 1 d before infection with vector stocks that were diluted 1:10 with Dulbecco's modified Eagle's medium (DME). Complete growth medium was added 1.5 h after infection, and the cells were incubated for an additional 48–52 h before use. Since the uptake of plasma membrane HA0 into the endocytic pathway of these cells was < 3%/h (47; Copeland, C., unpublished observations), the cell-associated HA0 was present primarily on the plasma membrane and in organelles of the exocytic pathway. The X:31 strain of influenza virus, derived from A/Aichi/1968, was propagated in embryonated eggs as described (16).

HA Preparations

BHA was prepared and radioiodinated as described (16). An additional sucrose velocity gradient centrifugation was used to remove free ^{125}I (24). [^{35}S]Methionine-labeled HA and HA0 were isolated from CV-1 cells infected with X:31 virus as described (15). Anchor minus HA0 was prepared from [^{35}S]methionine-labeled CV-1 cells infected with SVEXHA-A$^-$ as follows: Two 90-mm dishes of cells were infected as above using a 1:5 dilution of the vector stock. 51 h postinfection the monolayers were washed twice in methionine-free modified Eagle's minimum essential medium (MEM) containing 5% dialyzed fetal calf serum. [^{35}S]Methionine was added (1 mCi per dish in 4 ml of methionine-free MEM), and the incubation was continued for 23 h. Supernatants were collected, cell debris was removed by centrifugation, and protease inhibitors were added (1 mM phenylmethylsulfonyl fluoride [PMSF] and 0.1 trypsin inhibitor units [TIU] of aprotinin per ml). The [^{35}S]methionine-labeled anchor minus HA0 was purified by ricin-Sepharose affinity chromatography and by velocity gradient centrifugation as described for BHA (24).

Antibody Production

The polyclonal rabbit anti-HA serum was obtained after immunization with BHA and X:31 virus (16). Before use in this study the rabbit was boosted intravenously with 150 μg of pH 4.8-treated purified virus and bled 10 d later.

The conformation-specific mouse monoclonal antibodies 88/2 and 12/1 have been described previously (62). To obtain additional conformation-specific monoclonal antibodies, female CD2F1 mice were injected intraperitoneally with 50 μg of X:31 virus in morpholinoethanesulfonic acid (MES)-saline buffer (20 mM MES, 0.13 M NaCl, pH 7.0). The virus was either untreated or pretreated with low pH buffer (pH 4.8). 21 d later the injection was repeated, and 3 d later spleen cells from each mouse were fused separately to P3U1 mouse myeloma cells (61). After 2 w, supernatants of growing cultures were screened for the ability to immunoprecipitate the neutral and acid conformations of ^{125}I-BHA as described (16). Hybridomas of interest were picked, expanded, and subcloned twice in soft agar. Screening was repeated numerous times during cloning and expansion.

Ascites fluids containing monoclonal antibodies were produced by standard methods in female CD2F1 mice primed with pristane (8). Alternatively, culture supernatants from cells grown in DME/alpha MEM (1:1) with 1% Nutridoma-SP were used directly. The epitopes recognized by N1 and N2 were determined by hemagglutination inhibition using a panel of variant viruses as described (62).

Immunofluorescence

For immunofluorescence, sterile glass coverslips were placed in culture dishes before plating CV-1 cells. The standard infection procedure was followed, except that the volume of diluted vector was increased to 4 ml. Before fixation some coverslips were trypsinized as described below, washed with soybean trypsin inhibitor, and exposed to pH 4.8 MES-saline for 10 min at 37°C. Cells were reneutralized by washing in phosphate-buffered saline (PBS) and prepared for immunofluorescence essentially as described by Timm et al. (58), using 0.1% Triton X-100 (TX100) to permeabilize the cells. All PBS solutions were supplemented with $CaCl_2$ (1 mM) and $MgCl_2$ (0.5 mM). Nutridoma supernatants were diluted 1:2 to 1:10 and ascites fluid 1:100 to 1:200, depending on the antibody and preparation. Negligible staining of uninfected control cells was seen with the antibodies used.

Electron Microscopic Immunocytochemistry

Immunoperoxidase cytochemistry was performed following the procedure of Brown and Farquhar (7) with minor modifications. Fixation was in 0.01 M periodate, 2% (wt/vol) formaldehyde, 0.75 M lysine in 37.5 mM sodium phosphate pH 7.4 for 4 h directly on the culture dish. Cells on the culture dish were permeabilized with solution A (PBS, 0.1% ovalbumin, 0.005% saponin) for 15 min, then incubated in antibody 12/1 diluted 1:50 in buffer A for 1 h at room temperature. Dishes were washed in buffer A three times for 15 min. Peroxidase-conjugated sheep anti-mouse Fab fragments were added (diluted 1:50 in buffer A) and incubated for 1 h at room temperature. The plates were washed in buffer A (three times, 5 min each) and then in buffer A without saponin (three times, 15 min each). Cells were then fixed in 2.5% glutaraldehyde, 100 mM Na cacodylate, 5% sucrose for 1 h at room temperature. Peroxidase activity was visualized by incubation with diaminobenzidine (0.1%) and hydrogen peroxide (0.01%) in Tris buffer with 7.5% sucrose for 3–5 min at room temperature. Sections were stained in uranyl acetate and lead citrate, then examined in a JEOL 100-CX electron microscope operated at an accelerating voltage of 60 kV.

Metabolic Labeling and Pulse-Chase Protocols

Infected cells were washed twice with PBS and preincubated in methionine-free medium with 20 mM Hepes for 15 min at 37°C. [^{35}S]Methionine at 0.25 mCi/ml was added for 5 min at 37°C (0.25 mCi per 90-mm dish). Cells were washed once with prewarmed chase medium (DME, 10 mM methionine, 10 mM Hepes, 10% FCS) and then chased for various periods at 37°C. In some experiments cycloheximide (25–50 μg/ml) was added to the chase medium with no detectable effect on methionine incorporation or formation of the N2 epitope in HA0. At the end of the chase period, cells were washed twice with ice-cold PBS and kept on ice in PBS until all samples were ready. Cells were lysed by scraping in PBS containing 1% TX100, 0.1 TIU/ml aprotinin, 20 μg/ml soybean trypsin inhibitor, and 1 mM PMSF. The dishes were washed once with lysis buffer. The cell lysates were centrifuged for 5 min in a Brinkmann microfuge (Brinkmann Instruments Co., Westbury, NY), and the supernatants were adjusted to equal volumes. Aliquots were either frozen in liquid nitrogen and stored at −80°C, or used immediately.

Immunoprecipitation of HA0 from Cell Lysates

Goat anti-mouse IgG or goat anti-rabbit IgG (10 μl per sample) was added to prewashed, fixed *Staphylococcus aureus* (120 μl of a 10% slurry per sam-

ple), by incubation for 1–2 h at 4°C on a LabQuake shaker (Lab Industries, Berkeley, CA). The primary antibodies were added to these complexes (5 μl ascites fluid, 250 μl culture supernatant, or 15 μl rabbit serum per sample) and incubated as above for 1–2 h. The complexes were washed with PBS containing 0.5% TX100, resuspended, and aliquots were incubated with the cell lysates at 4°C for 1 h on an Eppendorf shaker. Washing of the immunoprecipitated material was according to Webster et al. (62) except for the polyclonal rabbit serum and antibody N2, for which the immunoprecipitation procedure of Mellman et al. (38) was used.

After the washes, the pellets were resuspended in buffer (10 mM Tris pH 6.8, 0.1 TIU/ml aprotinin, 1 mM PMSF, 1 mM EDTA). Sample buffer was added (final concentrations 200 mM Tris pH 6.8, 3% SDS, 10% glycerol, 20 mM dithiothreitol, 0.004% bromophenol blue, 1 mM EDTA), and the samples were heated to 95°C for 5 min. The *S. aureus* was removed by two sequential high speed centrifugations, and aliquots of the supernatant were used for SDS PAGE according to Laemmli (31) or for radioactivity determinations.

Fluorography was performed on gels impregnated with salicylic acid (11) using Kodak XAR-5 film preflashed with orange light. Densitometric scans were made using a Hoefer GS 350 scanning densitometer (Hoefer Scientific Instruments, San Francisco, CA), and integration was performed on an IBM personal computer (IBM Instruments, Inc., Danbury, CT) using Hoefer GS 350 densitometry software. Care was taken to ensure that exposures used for quantitation were within the linear range of the film.

Trypsin Digestion of Cell Surface and Intracellular HA0

For detection of HA0 at the cell surface (37), monolayers were trypsinized at the end of the chase period using tosylamidephenylethylchloromethyl ketone–treated trypsin (TPCK-trypsin) at 100 μg/ml in PBS for 30 min at 0°C. Trypsinization was terminated by two 5-min washes in soybean trypsin inhibitor (100 μg/ml in PBS) before lysis of cells for immunoprecipitation or sedimentation analysis in sucrose gradients. To calculate the time course of HA0 arrival at the plasma membrane, cells were lysed and immunoprecipitated with the polyclonal antiserum, as described above. After SDS PAGE, fluorography, and densitometry, the percentage of HA1 and HA2 relative to the total HA in the lane was calculated.

When cell lysates were trypsinized a somewhat different procedure was used. TPCK-trypsin was added to the lysates at a final concentration of 50 μg/ml in lysis buffer with 1 mM EDTA but without other protease inhibitors. To obtain complete cleavage of HA0 to HA1 and HA2, digestion was carried out for 30 min at 0°C. Digestion was terminated by adding soybean trypsin inhibitor, aprotinin, and PMSF at the final concentrations 200 μg/ml, 0.1 TIU/ml, and 1 mM, respectively. These inhibitors were shown to completely prevent cleavage of HA0 when added to cell lysates before trypsin.

Immunoblotting

Electrophoretic transfer of proteins from SDS polyacrylamide gels was performed according to Towbin et al. (59) with two modifications: the nitrocellulose sheet was boiled before transfer, and 0.1% TX100 was included in the wash buffer.

Sucrose Velocity Gradient Centrifugation

For velocity gradient sedimentation experiments using cell lysates, metabolic labeling of HA0 was performed as described above except that the lysis buffer used was 20 mM MES, 30 mM Tris, and 100 mM NaCl (MNT buffer) with 1% TX100. Nuclei and insoluble cytoskeleton components were removed by centrifugation for 5 min in a Brinkmann microfuge, and an aliquot of lysate was layered on top of a continuous 5–25% sucrose gradient in MNT with 0.1% TX100 overlaid on a 0.75-ml cushion of 60% sucrose. Centrifugation was for 16 h at 20°C in a Beckman SW40 rotor (Beckman Instruments, Inc., Palo Alto, CA) at 40,000 rpm. Gradients were fractionated by collecting drops from the punctured tube bottom. The sedimentation coefficients were determined using standard proteins, partially purified BHA, and HA0 as previously described (15). For sedimentation of BHA and anchor minus HA0, TX100 was omitted from the sucrose solutions.

Endoglycosidase H Digestion

In some cases samples for SDS PAGE were digested with endoglycosidase H (endo H) before electrophoresis. This enzyme cleaves asparagine-linked carbohydrates between the two most proximal N-acetyl glucosamine residues. Carbohydrate chains that have fucose or terminal sugars added, however, are no longer good substrates for endo H (57). Pellets after immunoprecipitation were heated to 95°C in SDS PAGE sample buffer, the *S. aureus* was removed, and the supernatants diluted 15-fold with 0.1 M Na acetate pH 6.0 (final SDS concentration, 0.2%). Protease inhibitors were added: antipain A, 2 μg/ml; pepstatin A, 4 μg/ml; aprotinin, 0.1 TIU/ml; PMSF, 1 mM. Then endo H was added (25 mU/ml final), and the samples were incubated for 16 h at 37°C. Samples were then precipitated with 10% TCA for 1 h at 0°C, washed twice with cold ethanol/ether (1:1), and resuspended for SDS PAGE as described above for immunoprecipitates.

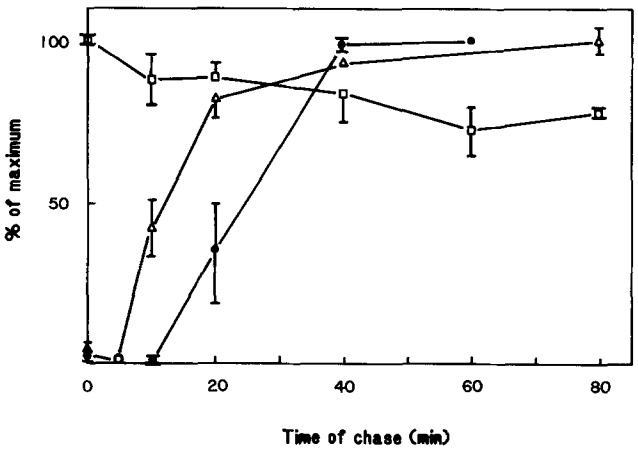

Figure 1. HA0 arrival at the plasma membrane and acquisition of endo H resistance in the Golgi complex. Cells were pulse-labeled for 5 min with [^{35}S]methionine and chased as indicated. Labeled cell surface HA0 (●) was assayed by trypsin cleavage on the cell surface followed by immunoprecipitation with the polyclonal antiserum, SDS PAGE, fluorography, and densitometry. To determine endo H resistance (△), HA0 was immunoprecipitated from untrypsinized cells by the polyclonal antiserum and digested with endo H. HA0 bands, detected by SDS PAGE and fluorography, were quantitated, and the percentage of HA0 resistant to endo H at each time point was determined. Cleavage and resistance are expressed as the percent of the maximum amount in each experiment. At 40 min of chase, 70% of total cell associated HA0 was cleaved to HA1 and HA2, and 89% was endo H resistant. □, [^{35}S]methionine counts precipitated by TCA from aliquots of lysates used for immunoprecipitation.

Reagents

The FITC-conjugated goat F(ab')$_2$ anti-mouse IgM + IgG, the goat anti-mouse IgG, and the goat anti-rabbit IgG, all affinity purified, were purchased from Tago Inc. (Burlingame, CA). Mice were purchased from Charles River Breeding Laboratories, Inc. (Wilmington, MA). Peroxidase-conjugated sheep anti-mouse Fab fragments were from BIO-SYS (Pasteur Institute, Paris). Fixed *S. aureus* was from Zymed (South San Francisco, CA), Nutridoma-SP was from Boehringer Mannheim Biochemicals (Indianapolis, IN), and endo H from Miles Scientific Div., Miles Laboratories Inc. (Naperville, IL). Cycloheximide was from Calbiochem-Behring Corp. (La Jolla, CA), and TPCK-trypsin and all protease inhibitors were from Sigma Chemical Co. (St. Louis, MO). [^{35}S]Methionine was purchased from Amersham Corp. (Arlington Heights, IL), and had a specific activity of >800 Ci/mmol (3.7×10^4 Ci/Becquerel). Na^{125}I was also from Amersham Corp. and had a specific activity of ~16 mCi/μg iodine. Iodogen was from Pierce Chemical Co. (Rockford, IL). All other chemicals were reagent grade.

Results

HA Synthesis and Transport

HA0 was expressed in CV-1 monkey kidney cells using an SV-40 vector (SVEXHA) containing the cDNA of the X:31

hemagglutinin (14, 18). To determine the kinetics of HA0 transport to the cell surface, the cells were given a 5-min pulse of [^{35}S]methionine followed by a 0–60 min chase. Labeled HA0 reaching the plasma membrane was assayed using trypsin digestion. Like most tissue culture cells, CV-1 cells lack the protease needed to cleave the HA0 precursor to its HA1 and HA2 subunits. However, trypsin added to the medium will perform the activating cleavage, thus providing a means for distinguishing between cell surface and intracellular HA0 (37). The cells were lysed with TX100 and subjected to immunoprecipitation using polyclonal anti-HA antibodies followed by SDS PAGE (see Materials and Methods). Fig. 1 shows the amount of labeled HA present on the cell surface at different times of chase, as determined by densitometric scanning of fluorograms. According to these results, HA0 began to appear on the surface ~20 min after synthesis and the amount increased with time until ~40 min. The amount delivered was 70–80% of the total HA0 synthesized during the pulse. Similar rates of transport to the plasma membrane have been previously reported by Matlin and Simons (37) and Rodriguez-Boulan et al. (46).

Fig. 1 also shows the TCA-precipitable [^{35}S]methionine activity in total protein at different times of chase. No further [^{35}S]methionine was incorporated into protein after the end of the pulse. The appearance of endo H-resistant HA0 has also been included in Fig. 1 to illustrate the kinetics by which HA0 passes through the medial and *trans* Golgi compartments (see below).

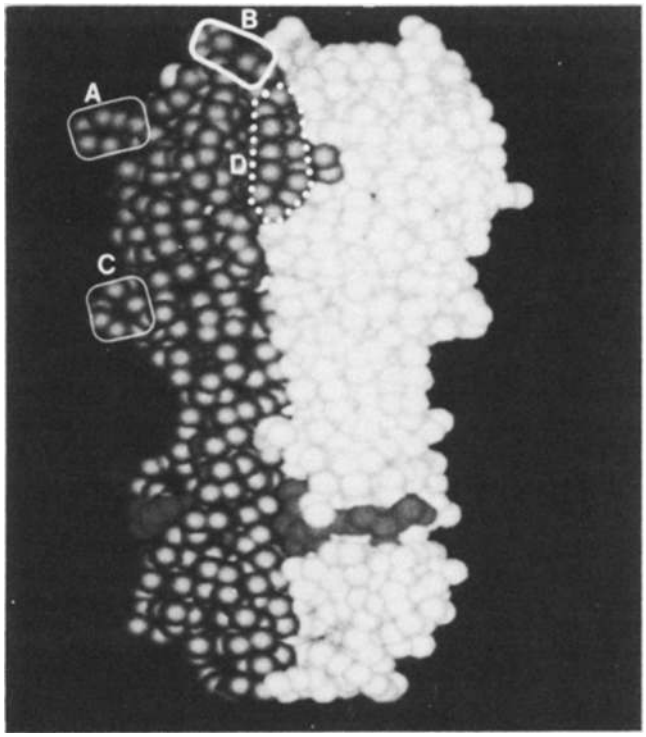

A: loop B: tip C: hinge D: interface

Figure 2. Antigenic sites on hemagglutinin. The crystal structure of BHA is depicted with the antibody binding sites marked. One of the subunits and the N-terminal peptides of HA2 are shown in darker color. The antibody-binding sites called *B* and *D* are located close to the interface between the HA1 top domains of the trimeric molecule, whereas sites *A* and *C* are far removed from the interface. The figure is based on a picture obtained from Drs. Don Wiley and Richard Feldman.

To monitor the formation of HA0 trimers, we used three approaches. First, we took advantage of the detailed information available on the nature of HA's antibody-binding sites, some of which could be shown to be present only on mature trimeric HA and HA0. Second, we determined the protease resistance of HA0, a property characteristic of mature HA and HA0 trimers but not of monomeric forms of the proteins (16, 49). Third, we used sucrose gradient centrifugation in the presence of nonionic detergent to separate intracellular trimeric from monomeric hemagglutinin. These approaches are described below beginning with the immunochemical experiments.

Antibodies against Monomeric and Trimeric HA0

The neutral pH conformations of HA and HA0 are known to have four antibody-binding regions, all located on the top domain of HA1 (Fig. 2 and references 21, 63, and 65). Two partially overlapping sites, called tip (or *B*) and interface (or *D*), are in or close to the interface between adjoining HA1 subunits. The ability of some monoclonal antibodies to bind to these sites is lost when the molecule undergoes the irreversible, acid-induced conformational change which accompanies activation of membrane fusion (12, 16, 27, 62, 67). In contrast, the loop (*A*), which is relatively distant from the trimer interface, is not appreciably affected by the conformational change. The acid form of HA also possesses unique antibody-binding sites. Antibodies to HA, therefore, fall into three categories: those that exclusively recognize the neutral form, those that recognize only the acid form, and those that recognize both forms. There is considerable evidence that the acid-induced conformational change in HA involves a partial dissociation of the HA trimer (for reviews see references 23 and 64). The top domains, which contain the antigenic epitopes, separate from each other by moving away from the central axis of the molecule (13, 16, 50).

The loss of antibody binding to epitopes B and D when the top domains move apart, suggested that these sites were dependent on the quaternary structure of hemagglutinin and thus are potentially useful for detecting trimers. To test this possibility, we established a panel of conformation-specific antibodies to HA. Two previously isolated antibodies, 12/1 and 88/2 (62), were complemented with the newly generated mouse monoclonal antibodies A1 and A2 (acid-specific), N1 and N2 (neutral-specific). The relevant properties and binding sites are summarized in Table I. The neutral-specific monoclonals N1 and N2 recognize the tip epitope (*B*), because they fail to bind to variant viruses with point mutations in this epitope. 12/1 has been previously characterized as binding to the tip/interface region of the hemagglutinin (62). Although the exact position of the epitopes for the acid-specific antibodies A1 and A2 could not be determined, immunoblotting showed that they recognized HA2 and HA1 polypeptides, respectively (not shown). The acid-specific monoclonal antibody 88/2 reacts with an epitope in HA1 (Table I and reference 27). In addition to these monoclonal antibodies, we made use of a polyclonal rabbit anti-HA serum (raised against both low pH and neutral pH influenza virus), which precipitated acid and neutral forms of HA and HA0 equally well. It is noteworthy that this is the only rabbit se-

Table 1. Specificity of Anti-hemagglutinin Antibodies

Antibody	Epitope	Reactivity assay by immunoprecipitation* (cpm precipitated) HA pH 7	HA pH 5	HA0 pH 7	Anchor minus HA0, pH 7
Neutral-specific monoclonals					
N1	HA1 tip (B)	12,327	799	17,430	0‡
N2	HA1 tip (B)	13,360	674	13,802	0‡
12/1§	HA1 tip interface (B/D)	10,107	297	ND‖	0‡
Acid-specific monoclonals					
A1	HA2	58	11,991	1,336	9,006
A2	HA1	222	14,485	1,145	6,879
88/2§	HA1	68	3,123	42	6,056
Conformation-independent polyclonal antiserum					
	HA1 + HA2	13,695	11,472	17,039	14,856

* [^{35}S] Methionine-labeled hemagglutinin proteins were prepared as described in Materials and Methods, and immunoprecipitated with the different antibodies by the procedure described for the hybridoma screening. Low pH-treated proteins were reneutralized before precipitation. Approximately 20,000 cpm of labeled protein was used for each precipitation. A background of nonspecific precipitation is subtracted.
‡ Less than background with nonspecific antibody.
§ Previously described by Webster et al. (62).
‖ ND, not done.

rum we have tested that can precipitate ER forms of HA0 to the same extent as the mature HA0 (see Fig. 6, below).

To determine whether any of the neutral-specific antibodies were indeed specific for trimers, we tested their ability to immunoprecipitate trimeric and monomeric HA0. A monomeric form of HA0 was obtained by expressing a truncated hemagglutinin gene lacking the carboxy-terminal membrane anchor. Anchor minus HA0, the product of this gene, is secreted into the extracellular medium as a soluble protein and is easily purified (26). When subjected to sucrose velocity gradient centrifugation it was found that most of the anchor minus HA0 sedimented with a sedimentation coefficient of ~4.3S (Fig. 3), which showed that it was monomeric (Doms, R., M.-J. Gething, J. Sambrook, and A. Helenius, manuscript in preparation). In contrast, mature wild-type HA0 sedimented as 9S complexes (Fig. 10) as previously shown (15, 33).

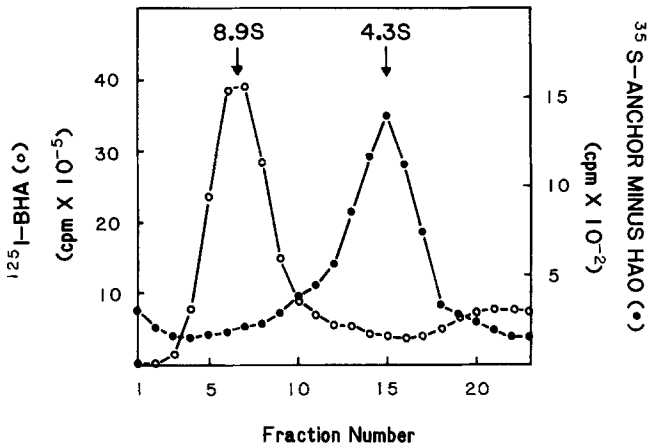

Figure 3. Sedimentation analysis of anchor minus HA0. Anchor minus HA0, labeled with [^{35}S]methionine (•), was subjected to sucrose velocity gradient centrifugation as described in the Materials and Methods. BHA, labeled with ^{125}I (o), was run as a marker on an identical gradient. Fractions are numbered starting with the bottom of the tube.

Immunoprecipitation analysis showed that [^{35}S]methionine-labeled anchor minus HA0 reacted with the acid-specific monoclonal antibodies A1, A2, and 88/2, and with the conformation-independent polyclonal antiserum. Although these acid-specific antibodies can recognize this particular form of monomeric HA0, they apparently did not detect intracellular HA0 monomers which are precursors to the mature trimer (see Fig. 6 *a* for antibody A1, data not shown for antibodies A2 and 88/2). Furthermore, since the pH 5 conformation of HA is known to be trimeric (15), these antibodies are not solely monomer-specific, but recognize epitopes that are masked in the mature trimer.

In contrast to the results with the acid-specific antibodies, the neutral-specific antibodies failed to react with anchor minus HA0 monomers (Table I). Thus, the neutral-specific antibodies could be used to distinguish between monomeric and trimeric forms of HA0 that had not previously been exposed to acid.

Immunofluorescence Analysis of Cells Expressing HA0

The antibodies were next used to determine the cellular distribution of HA0 by indirect immunofluorescence. The cells in *a–c* of Fig. 4 were labeled with the neutral-specific antibody N2, and the cells in *d–f* with the acid-specific antibody A1. Hemagglutinin could be clearly visualized on the cell surface with either antibody, provided that it was in the appropriate conformation. Without prior acid treatment (*a* and *d*) the cells could be stained with N2 but not with A1. The opposite pattern was observed if the HA0 was trypsinized and briefly acidified (*b* and *e*).

When cells were permeabilized with TX100 to allow access of antibodies to intracellular HA0, a different staining pattern emerged (*c* and *f*). The acid-specific antibody A1 gave a strong reticular staining throughout the cytoplasm as

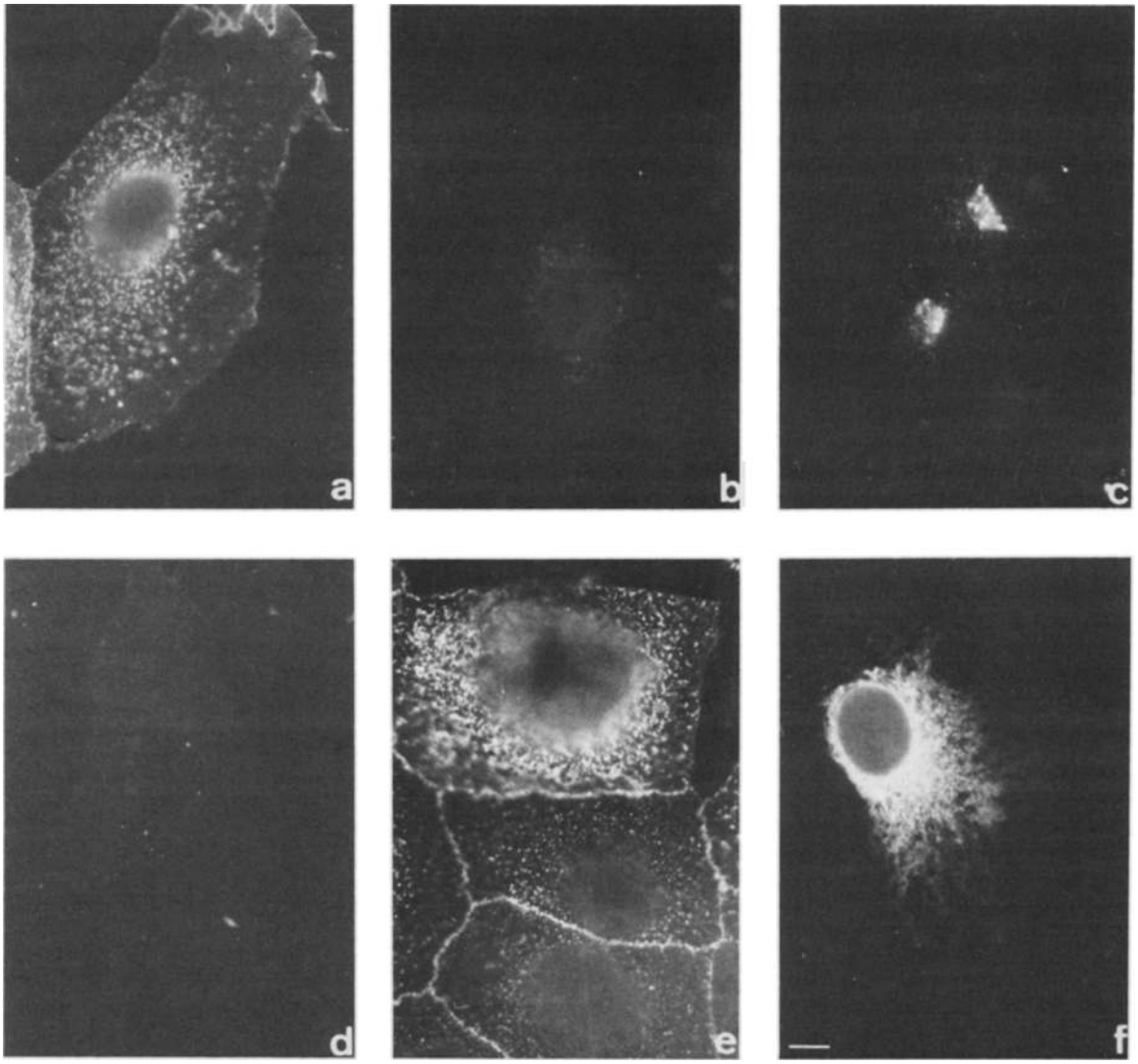

Figure 4. Immunofluorescence staining of hemagglutinin-expressing CV-1 cells with conformation-specific antibodies. Cells in *a–c* were stained with the neutral-specific antibody N2 and cells in *d–f* with the acid-specific antibody A1. Surface staining was performed without (*a* and *d*) or with (*b* and *e*) prior treatment with trypsin and low pH to convert plasma membrane HA0 into the low pH conformation. Internal staining is shown in *c* and *f*. For internal staining with N2 (*c*), the surface HA0 was also converted to low pH HA, so that internal organelles could be visualized without an interfering surface fluorescence. Bar, 10 μm.

well as occasional staining of the nuclear envelope (*f*). This staining pattern is typical of ER markers (34), and has been observed previously by Bächi et al. (4) using another acid-HA specific antibody. To determine the intracellular distribution of HA0 possessing neutral epitopes, the cells were trypsinized, acidified, and reneutralized before fixation. This treatment effectively removed the surface staining with N2 (*b*), N1, and 12/1 (not shown). The internal labeling pattern observed after permeabilization (Fig. 4 *c*) was different from that obtained for the acid-specific antibody (Fig. 4 *f*). Antibody N1 stained dense accumulations of vacuoles in the perinuclear area of the cells, a staining pattern characteristic of the Golgi complex (34). In addition, smaller vesicular structures throughout the cytoplasm were stained.

The intracellular distribution of HA0 reacting with the neutral-specific antibody 12/1 was investigated using ultrastructural immunocytochemistry in saponin-treated cells. As shown in Fig. 5, this antibody stained mainly the cisternae of the Golgi complexes and some cytoplasmic vacuoles. The plasma membrane was also heavily stained (not shown). The morphological analyses suggested that intracellular HA0 occurred in at least two conformational states and that the two populations of hemagglutinin were located in different organelles. The ER contained a form detected by the acid-specific monoclonal antibody, whereas the Golgi complexes, cytoplasmic vacuoles, and plasma membrane contained HA0 mainly in the neutral, trimeric conformation.

Immunoprecipitation Analysis

To determine whether the differential localization was caused by antigenic changes in HA0 during intracellular transport, we performed immunoprecipitations with the conformation-specific antibodies. CV-1 cells expressing HA0 were pulse-labeled with [^{35}S]methionine for 5 min and chased for various times. Immunoprecipitation, SDS PAGE,

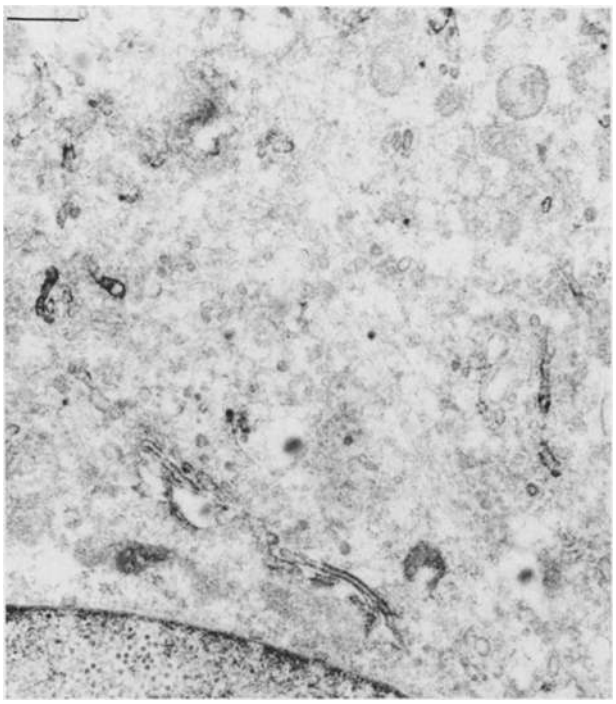

Figure 5. Electron microscopic immunocytochemistry with a neutral-specific antibody. Lightly fixed CV-1 cells expressing HA0 were permeabilized, stained with antibody 12/1, and processed for immunocytochemistry by the indirect immunoperoxidase method. Dense reaction product is visible within the cisternae of the Golgi apparatus and in small vesicles. Bar, 0.5 μm.

fluorography, and quantitation of gel bands were then carried out as described in Materials and Methods. Fig. 6 *a* shows a fluorograph obtained using the polyclonal rabbit serum and the monoclonal antibodies N2 and A1. Fig. 6 *b* presents the averaged densitometric results from three experiments. At 0 min of chase the polyclonal rabbit serum recognized a labeled HA0 species that migrated with a mobility in our gel system of ~80 kD. A slight shift to faster mobility was seen in the band precipitated after 5 and 10 min of chase, followed by a shift to slower mobility at 20 min. The first, downward, shift was most likely caused by trimming of the mannose-rich N-linked sugar chains (5) and the second, upward, shift by terminal glycosylation (37).

The neutral-specific antibody N2 precipitated a small amount of the HA0 present at 0 min chase. By 5 min into the chase, the amount of HA0 precipitated by N2 had begun to increase and by 10 min almost as much HA0 was precipitated as with the polyclonal antibody. Thereafter the amount of HA0 remained approximately constant with time. Since no further incorporation of [^{35}S]methionine into protein took place after the beginning of the chase (Fig. 1), the change in immunoreactivity with N2 must correspond to a posttranslational change in HA0. Because the pulse was 5-min long and half maximal precipitation with N2 was observed after ~5 min of chase, we estimated that a half-time for the appearance of the epitope was ~7–8 min after synthesis. When the lysates were subjected to a second round of immunoprecipitation with this antibody, no further HA0 was recovered, indicating that precipitation was quantitative. (Quantitative

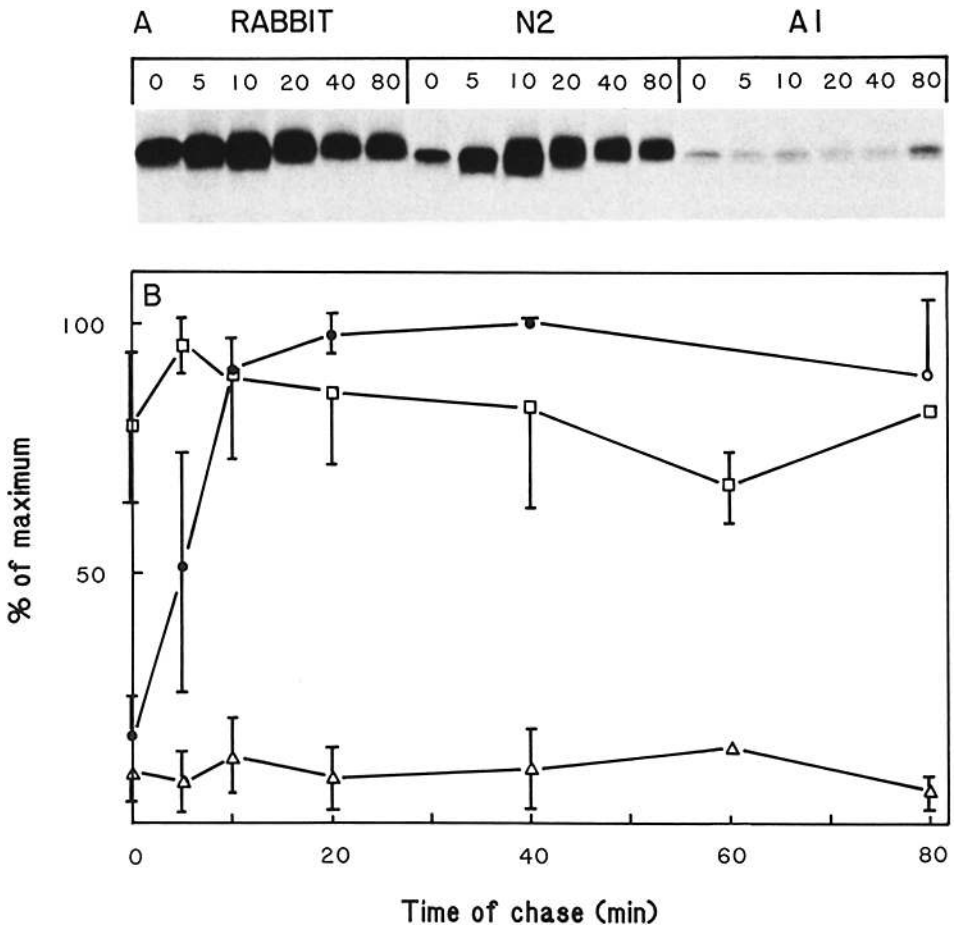

Figure 6. Immunoprecipitation of pulse-chase labeled cells using conformation-specific antibodies. (*a*) CV-1 cells expressing HA0 were labeled for 5 min with [^{35}S]methionine, chased for 0–80 min as indicated above each lane, and immunoprecipitated with the polyclonal rabbit serum, the neutral-specific antibody N2, or the acid-specific antibody A1. The immunoprecipitates were subjected to SDS PAGE and fluorography. (*b*) Fluorographs of three experiments like that shown in *a* were used for scanning densitometry to determine the intensity of HA0 bands precipitated by N2 (●), A1 (△), and the rabbit serum (□). For each experiment, the intensities of the bands were normalized to the highest amount of HA0 detected (% of maximum), and the normalized values were averaged.

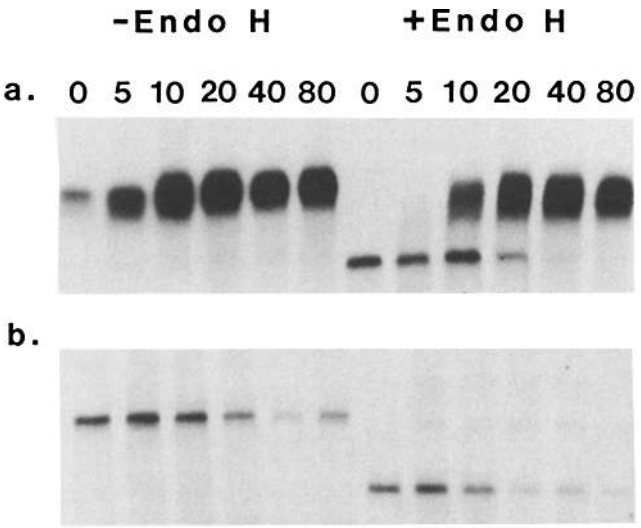

Figure 7. Endo H digestion of HA0 precipitated with N2 or A1. Cells expressing HA0 were pulse-labeled and chased for the indicated time (0–80 min), and lysates were immunoprecipitated with antibody N2 (*a*) or A1 (*b*). To digest the high-mannose oligosaccharides, immunoprecipitated material was incubated in the presence of endoglycosidase H (lanes *+Endo H*). Control incubations were carried out without enzyme (lanes *−Endo H*).

precipitation was also observed with the other antibodies used in this study.) Large increases in reactivity after 5–10 min of chase were also detected with 12/1 and N1 (not shown).

The HA0 recognized by N2 underwent the changes in mobility attributed to carbohydrate trimming and terminal glycosylation seen in HA0 reacting with the polyclonal serum (Figs. 6 and 7 *a*). Because trimming reactions are known to begin in the ER and continue in the proximal cisternae of the Golgi complex (29), the formation of the neutral epitope can be assigned to a time point just before, during, or just after the movement of HA0 between the two organelles, but well before terminal glycosylation which occurs in *trans* cisternae of the Golgi apparatus.

To confirm this finding, we subjected aliquots of the immunoprecipitated HA0 samples to digestion with endo H, an enzyme that removes N-linked carbohydrate chains that have not been terminally glycosylated (57). The transition of a glycoprotein's carbohydrates to endo H resistance is widely accepted as a marker for transport of the protein into or past the medial elements of the Golgi complex (19). The HA0 immunoprecipitated with N2 was initially sensitive to endo H, acquiring resistance between 10 and 20 min of chase time (Fig. 7 *a*, see also Fig. 1 for results with the polyclonal antiserum). This result indicated that N2 recognizes HA0 well before it has reached the medial or *trans* Golgi complex.

The patterns observed with the acid-specific antibody A1 were quite different (Figs. 6 and 7 *b*). Irrespective of chase time, only a small amount of HA0 was precipitated. On SDS gels a double band was seen, which represented ~10% of total HA0 synthesized. Neither of the bands in the doublet shifted position on the gel during the chase, suggesting that the carbohydrate chains were neither trimmed nor modified to complex chains. This was confirmed by the effects of endo H; the HA0 recognized by A1 did not become progressively resistant to the enzyme with time (Fig. 7 *b*). Interestingly, the lower band of the doublet appeared to be resistant to endo H at all times of chase. Because it is apparently not N-glycosylated, this protein may not be HA0. Recently, Gething et al. have shown that immunoglobulin heavy chain binding protein (BIP), an ER protein that is known not to be glycosylated, is associated with an incompletely folded form of hemagglutinin (25).

Taken together, the results indicated the epitope recognized by N2 appeared just before or at the time HA0 moves from the ER to the Golgi apparatus, suggesting that this is the time when trimerization occurs. The acid-specific antibody A1 did not detect an intracellular precursor to HA0 trimers, but rather a small amount of newly synthesized HA0 that apparently did not exit from the ER. This subpopulation of HA0 did not acquire the neutral-specific epitope. This material may accumulate in the ER, possibly explaining the strong straining detected by immunofluorescence with A1.

Trypsin Resistance of Newly Synthesized HA0

As an independent method of assessing the conformations of HA0, we subjected detergent lysates of pulse labeled HA0-expressing cells to digestion with trypsin. Mature trimeric HA is resistant to many proteases, and the same is true for HA0 which is only cleaved at the activating site, yielding HA1 and HA2. Acid-treated forms of hemagglutinin are, in contrast, very sensitive to trypsin and other proteases (16, 49) as is monomeric anchor minus HA0 (Doms, R., unpublished observations). Resistance to proteases seems, therefore, to

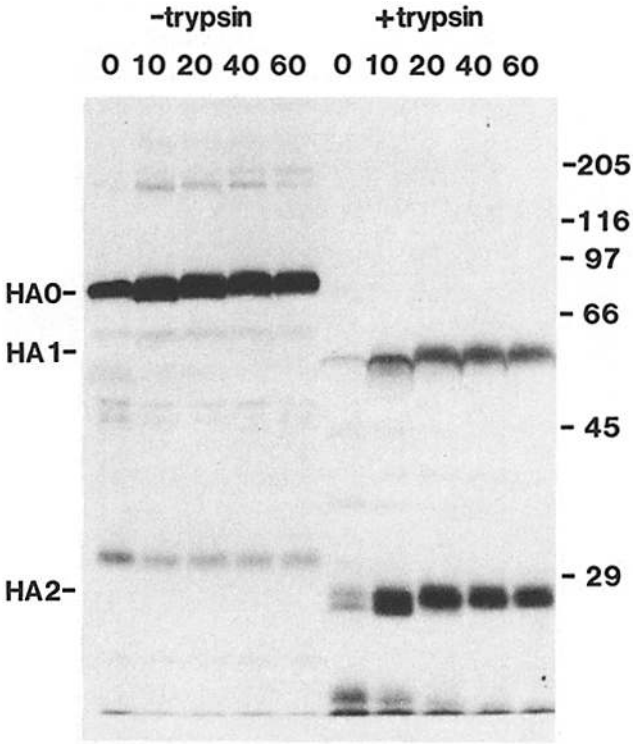

Figure 8. Trypsin digestion of HA0 in cell lysates. Pulse-chase labeling of CV-1 cells expressing HA0 was performed as in previous experiments. Cells were lysed with 1% TX100 in PBS and incubated for 30 min at 0°C in the presence or absence of trypsin. Excess protease inhibitors were then added and the lysates were immunoprecipitated with the polyclonal rabbit anti-HA serum. The numbers above each lane indicate the time of chase in minutes.

be an exclusive characteristic of HA and HA0 trimers in their neutral conformation.

Our results, shown in Fig. 8, demonstrated that ~70% of the HA0 labeled with a 5-min pulse was degraded by trypsin to fragments no longer precipitable by our polyclonal anti-HA serum. Approximately 30% of the HA0 synthesized in the pulse was recovered as HA1 and HA2. After chase, increasing label was seen in the HA1 and HA2 bands, indicating that additional HA0 had acquired trypsin resistance. Control samples in which trypsin was omitted showed minimal cleavage (Fig. 8). The quantitative analyses from two experiments showed that approximately half of the HA0 acquired trypsin resistance after 5 min of chase. This time course was nearly identical to that observed for the appearance of the neutral-specific epitopes as shown in Fig. 6 *b*. Trypsin cleavage sites are thus masked at the same time that the tip epitope is formed by the interaction of two or more subunits.

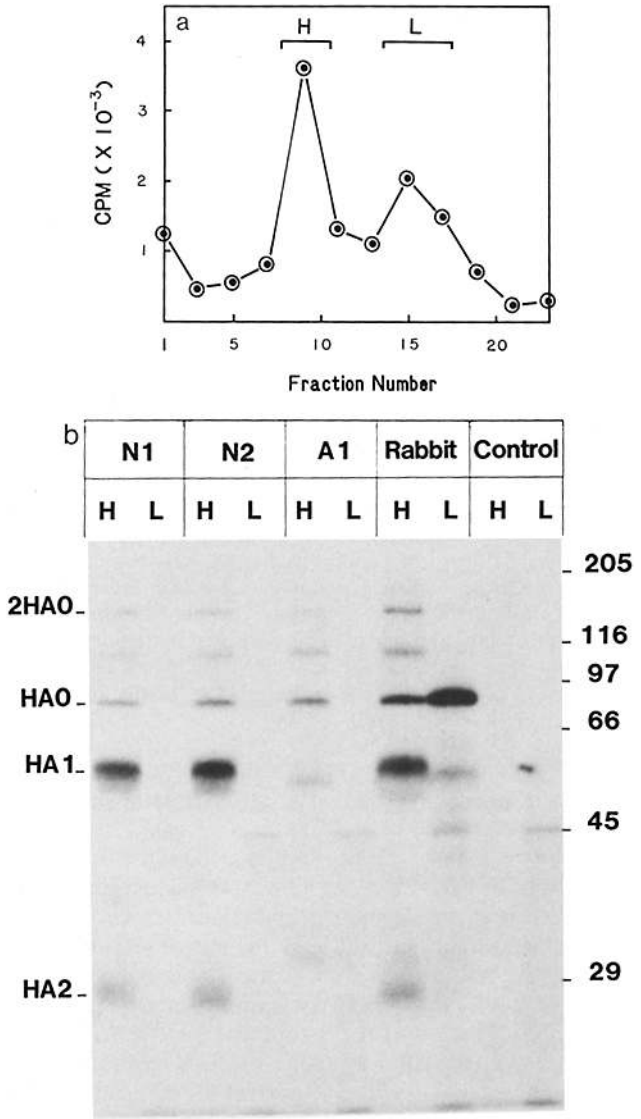

Figure 9. Sucrose velocity gradient sedimentation of metabolically labeled HA0. (*a*) Detergent lysates were prepared from HA0-expressing cells that were either pulse labeled for 5 min or pulse-labeled and chased for 75 min. Before lysis, the cells were trypsinized to convert cell surface HA0 to HA1 and HA2. The two lysates were mixed and subjected to sucrose velocity gradient centrifugation in the presence of TX100 as described in Materials and Methods. Alternate gradient fractions were immunoprecipitated with the polyclonal antiserum and aliquots of the precipitates were counted directly or used for SDS PAGE and fluorography (not shown). Fraction numbers are from the bottom of the tube. (*b*) The peak fractions of hemagglutinin from the gradient were pooled as indicated in *a* (*H* and *L*). The pools were then immunoprecipitated with the indicated antibodies, and the precipitates were subjected to SDS PAGE and fluorography. The positions of HA0, HA1, and HA2, as well as marker proteins are shown (molecular mass given in kilodaltons). 2HA0 indicates the position of dimeric HA0 which is incompletely dissociated by SDS treatment.

Velocity Sedimentation of Solubilized HA0

Isolated HA and HA0, solubilized by TX100, sediment in sucrose velocity gradients with a coefficient of $9S_{20,w}$ (15). Dimers and monomers have sedimentation coefficients of 7.7S and 4.5S, respectively. To determine whether monomeric and trimeric forms of cell-associated HA could be separated after solubilization with TX100, two dishes of cells were labeled with [^{35}S] methionine for 5 min. One was immediately placed on ice and the other was chased for 75 min before cooling. Both dishes were treated with trypsin to convert cell surface HA0 to HA. TX100 lysates prepared from the two plates were mixed with each other and loaded on a sucrose velocity gradient that contained 0.1% TX100. After centrifugation, alternate gradient fractions were immunoprecipitated with the conformation-independent polyclonal antibody. Half of the immunoprecipitated material was used for a determination of radioactivity, and the other half was subjected to SDS PAGE and fluorography.

As shown in Fig. 9 *a*, hemagglutinin was detected by the polyclonal antiserum in two peaks. The heavier peak sedimented slightly faster than marker HA0 (not shown) and had an apparent sedimentation coefficient of $9.1S_{20,w}$. The lighter peak was broader, including material with sedimentation coefficients in the 3.9–5.2S range. The heavy peak (*H*) contained virtually all the cell surface HA as indicated by the presence of HA1 and HA2 bands (Fig. 9 *b*, lane *rabbit H*). This confirmed that hemagglutinin on the plasma membrane was trimeric. In addition, the heavy peak contained a small amount of HA0, which represented intracellular trimers. A large HA0 band was seen in the broad, light peak (*L*), indicating the presence of an intracellular, monomeric HA0 population (Fig. 9 *b*). The minor amount of HA1 and HA2 seen in this peak was not reproducibly detected and probably resulted from some HA0 cleavage during the 16-h centrifugation at 20°C. Immunoprecipitations from the heavy peaks also contained a band of ~110 kD, which was not recognized by the control antibody. The identity of this protein is not yet known.

The fractions containing the monomer (*L*) and trimer (*H*) peaks were each pooled and immunoprecipitated with the monoclonal antibodies to correlate the antigenic structure with the oligomeric structure. The neutral-specific antibodies N1 and N2 reacted only with HA0 and HA in the 9.1S peak, confirming that these antibodies were trimer specific (see Table I, Fig. 3). Surprisingly, the acid-specific antibody A1 did not precipitate monomeric HA0, but did bring down a small amount of HA0 from the trimer peak. This antibody precipitated almost no cell surface HA1 or HA2 forms, indi-

cating that the small population of HA0 with the A1 epitope could not reach the plasma membrane. This was consistent with the lack of surface staining with A1 by immunofluorescence (Fig. 4 *d*) and the endo H sensitivity of this antigen (Fig. 7 *b*).

Kinetics of Complex Formation

We next investigated the sedimentation pattern of newly synthesized HA0 at different chase times. When a lysate of cells that had been pulse labeled but not chased was run on a sucrose velocity gradient, the main peak was at the position of monomeric HA0 (Fig. 10, 0 min). A small shoulder of activity was also seen, indicating the presence of some faster sedimenting forms. After 5 and 10 min of chase, the bulk of the HA0 still sedimented in the monomeric peak, although a more definite shoulder was apparent in the fractions containing trimers. By 40 min of chase almost all of the HA0 had shifted to the trimer peak. The time course of this shift was the same in three separate experiments.

The formation of trimers stable to the conditions of the centrifugation experiment therefore took place much later than the initial subunit interactions as assayed by both the antibody and trypsin. It is known for other membrane proteins that sucrose increases the likelihood of oligomer dissociation by TX100 (54). Therefore, the lack of sucrose and the low temperature used in the immunoprecipitation and trypsin digestions may explain why the complexes remained intact in TX100 during these experiments. The combined results suggest that, whereas initial association between HA0 subunits begins within the 5-min pulse and is complete by 10 min of chase, the formation of stable complexes that withstand the long centrifugation in at 20°C, takes considerably longer. HA0, therefore, undergoes two intracellular conformational changes. Indeed, the final, stable HA0 conformation may only be found once the HA0 has left the Golgi complex.

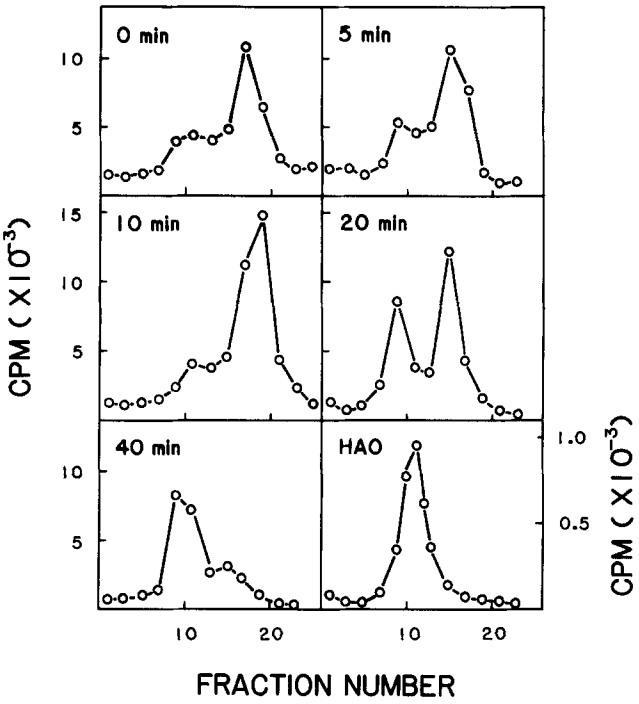

Figure 10. Sedimentation of HA0 at different times in intracellular transport. Cells expressing HA0 were pulse labeled, chased for 0–40 min, and lysed in TX100. Each lysate was then centrifuged through a sucrose gradient containing TX100 as in Fig. 9. Hemagglutinin was immunoprecipitated from gradient fractions with the polyclonal rabbit serum and aliquots were used for radioactivity determinations or for SDS PAGE and fluorography (not shown). The lower right panel shows the sedimentation profile of purified [^{35}S]methionine-labeled HA0.

Discussion

Subunit Interactions in HA

The extensive structural information available about influenza HA is a major advantage for studying the oligomerization process. The crystal structure of BHA shows that the trimeric ectodomain possesses two distinct parts; a head region composed of three independently folded globular HA1 domains and a stem region composed predominantly of HA2 chains from the three subunits (66). Polar and non-polar interactions between the three long alpha-helices of the stem provide the main forces stabilizing the trimer. Indeed, variant hemagglutinins which lack any one of a number of interchain salt bridges in this long triple-stranded coiled-coil stem are more sensitive to the dissociative effects of acid pH (13–15). Quaternary interactions between the globular top domains are fewer and less likely to play a central role in trimerization. Based on the crystal structure, Wilson et al. (66) have proposed that the top domains may, in fact, have folded already in the nascent chains before the signal peptide is cleaved off. These authors further suggested that because one face of the long alpha-helix is highly hydrophobic a single, folded subunit would be unlikely to project from the membrane as an erect spike. Although the individual subunits may fold independently of each other, a structural rearrangement is thus likely to occur at the time of subunit association.

Unlike the top and the stem regions, the x-ray structure is not known for the carboxy-terminal transmembrane domain of HA. This region of the molecule does, however, appear to be important for the stability of the mature trimer. Recent studies have shown that BHA, which lacks membrane anchors, is readily dissociated by acid treatment (15, 40) and by SDS denaturation (15). In contrast, intact HA is highly resistant to dissociation by either of these treatments. The membrane anchors are also important for efficient postsynthetic trimerization. When truncated hemagglutinin genes lacking the sequences encoding the transmembrane domain were expressed from SV-40 vectors, only a fraction of the resulting anchor minus HA0 was trimeric (Fig. 3; Doms, R., M.-J. Gething, J. Sambrook, and A. Helenius, unpublished results). The role of the membrane anchors in trimer assembly is probably twofold: they may orient the subunits in the membrane thereby facilitating assembly, and they may interact with each other and thus contribute to the stability of the final complex (15).

Assembly of HA0 Trimers

Our present observations show that the fully assembled HA0 is formed as a result of at least three posttranslational steps that affect subunit interactions: (*a*) Initial association between subunits within a few minutes after synthesis, (*b*) a

later event that renders the trimer stable to long term centrifugation in sucrose gradients containing TX100, and (*c*) the proteolytic cleavage which converts the HA0 trimer into mature HA.

Initial assembly was detected by the appearance of trimer-specific antigenic epitopes and by the acquisition of trypsin resistance. Both changes occurred with a $t_{1/2}$ of ~7–8 min after completion of synthesis of HA0. The tip (*B*) antibody-binding region, where the epitopes were located, is situated close to the subunit interface at the top of the trimer (Fig. 2, reference 65), as is one of two trypsin cleavage sites (residue 224) identified in acid-treated BHA (49). The second trypsin cleavage site, at position 28 in HA1, is near the central core of the molecule, midway down the stem (49). Examination of the x-ray structure shows that both of these cleavage sites are masked in the mature trimer. Since, during initial assembly, the epitopes become expressed and the trypsin sites are masked, we can assume that the top domains of the HA0 trimer and the stem reach a conformation and quaternary structure similar to that in mature trimers. The structure differs, however, from mature HA0 trimers in being less stable.

The HA0 trimers acquired full stability only 20–30 min after synthesis. If the top and middle regions are indeed already correctly assembled at this time, the stabilization event may involve a change primarily at the base of the spike or in the transmembrane anchors. As discussed above these regions of the molecule are important for stabilizing the trimer against dissociation.

The proteolytic cleavage that converts the HA0 to mature HA also must induce a significant conformational change in the lower part of the stem, because the amino terminus of HA2 thus created is 2.1 nm from the carboxyl terminus of HA1 (66). In cells that have the appropriate proteases this cleavage step occurs just before or at the moment of insertion into the plasma membrane (37). It probably constitutes a final modification in the hemagglutinin trimer.

Cellular Location of the Assembly Steps

Immunocytochemical and biochemical experiments allowed us to determine the organelles of the exocytic pathway in which the changes in oligomeric structure took place. Although no detectable staining of HA0 with trimer-specific antibodies was seen in the ER by morphologic methods, a small but clearly identifiable amount of HA0 possessing untrimmed N-linked carbohydrate side chains was immunoprecipitated with neutral-specific antibodies at early times of chase. A similar amount of newly synthesized HA0 was found to be trypsin resistant at this time. Therefore, initial trimerization probably takes place in the ER. Since the fraction of untrimmed HA0 recognized by the trimer-specific antibodies remained relatively low, oligomerization was probably followed by rapid transport of the complexes to the *cis* Golgi complex where trimming of the carbohydrate chains was completed. Without further evidence we cannot, however, exclude the possibility that oligomerization actually occurred in transit to or immediately upon arrival in the Golgi complex.

The second structural modification of HA0, which rendered it stable to long-term centrifugation, took place after HA0 had acquired endo H resistance. Half maximal conversion was observed about 20 min after synthesis. The stabilization of the trimers thus occurred late in the Golgi complex or in transit from the Golgi complex to the plasma membrane.

The general picture emerging from these results, and from similar data obtained by Gething and co-workers (25), indicates that assembly of HA0 trimers begins in the ER a few minutes after completion of translation. Thus HA0 monomers must exist transiently in the ER, but remained undetected in the present experiments. Initially the subunits seem to be assembled in such a way that the top domains and the stem regions interact. A further adjustment, which probably involves the lower part of the trimer, takes place in *trans* Golgi complex or later. In cells that contain the appropriate proteases this is followed by the activating cleavage. To what extent the numerous covalent posttranslational modifications (disulfide bond formation, carbohydrate modification, fatty acylation, and sulfation) are important in these events will be determined in future experiments.

The Role of Quaternary Structure in Transport

Although our results suggest that initial assembly begins at a time just before the HA0 moves from the ER to the Golgi complex, we cannot conclude with certainty from our present data that the assembly is a prerequisite for transport. Some independent event could, in principle, initiate both assembly and transport. Several reports in other systems have, however, indicated that subunit assembly may be a key factor in allowing transport of proteins to the plasma membrane (3, 10, 21, 22). Subunits of some newly synthesized plasma membrane and secretory proteins are known to remain in the ER if the appropriate subunits or co-factors are not available. This is illustrated by studies on the secretory proteins immunoglobulin (6), retinol-binding protein (45) and laminin (43). Observations on transmembrane proteins such as the class I histocompatibility antigens (3, 41, 53) and the LFA-1 and Mac-1 leukocyte antigens (55) suggest a similar effect. The nicotinic acetylcholine receptor, another membrane glycoprotein, is known, like HA0, to pass through at least two discrete intracellular conformations en route to the plasma membrane (9). The early change is detected by an increase in the affinity of the alpha subunit for a ligand, bungarotoxin. The second change involves a stable association between the alpha- and beta-subunits in velocity sedimentation experiments, and it may regulate surface delivery of the receptor (10). Cases in which quaternary interactions seem to play an important role in regulating efficiency of transport and sorting are also known in the endocytic pathway. Some cell surface receptors are more rapidly internalized as ligand receptor complexes than unoccupied receptors (56). In the case of the Fc receptor in macrophages it is known that the aggregation state of the receptor determines whether the protein is recycled from endosomes to the cell surface or routed with the ligand to the lysosomes (60).

There are, however, also reports showing that subunits can be transported out of the ER without forming the normal types of oligomeric interactions. For example, the p62 subunit of the Semliki Forest virus spike glycoprotein can be transported to the cell surface without the E1 subunit (28). Another case has been described for H-2D antigens (44). It is apparent that some proteins do not need the presence of their companion subunits to be transported.

The Aberrant ER Form of HA0

In addition to the pool of HA0, which is efficiently and rapidly transported along the secretory pathway, our results revealed the presence of a small conformationally altered population which remained resident in the ER. This form of HA0 was recognized by antibody A1 which binds to an epitope that is normally masked in the mature, neutral conformation of hemagglutinin. We do not believe that this population of HA0 arises from exposure to low pH in the ER for two reasons. First morphologic dyes which stain acidic compartments fail to stain the ER (2, 52). Second, the population constituted only ~10% of total HA0 synthesized. The results of the pulse-chase experiment ruled out the possibility that this population of HA0 was a precursor to mature trimeric HA0. The intracellular form of HA0 precipitated by A1 represented a population of HA0 molecules that were trimeric but somehow incorrectly folded.

While the exact nature of this aberrant trimeric HA0 remains unclear, its fate in the cell may point to a principle of general importance: oligomerization alone is not sufficient to allow transport of HA0 out of the ER. To be transported the assembled oligomers must have the correct conformation. This may explain why a variety of membrane proteins, with mutations in different domains, are inefficiently transported from the ER and through the Golgi complex (for reviews see references 20 and 48). A common property of the mutant proteins may be that they either do not assemble at all into oligomeric forms, or that they do assemble but the subunits are incorrectly folded. It is thus likely that the overall conformation of a protein is the determining factor for transport. In the case of multimeric proteins the overall conformation may critically depend on quaternary interactions. Further comparison of wild-type and mutant forms of the influenza HA0 may prove valuable in determining exactly where the line is drawn between the correct and incorrect forms.

An interesting question raised by these results concerns the nature of the cellular mechanism that distinguishes monomeric or incorrectly folded HA0 from the correctly assembled and folded proteins. Bole et al. (6) have shown that a specific ER protein (78 kD) called BIP is responsible for retaining unassembled forms of immunoglobulin in the ER. Gething et al. (25) have recently obtained direct evidence that BIP associates with incorrectly folded HA0 molecules. Another protein, egasyn, has been shown to retain the lysosomal enzyme betaglucuronidase in the ER of certain mouse strains (35). In view of these examples it may be suggested that specific host cell factors, such as BIP, are responsible for preventing the transport of misfolded and unassembled HA0 from the ER to the Golgi complex. Similar controlling factors may exist in the other stations of the intracellular pathway. The series of structural alterations that HA0 trimers undergo in passage to the cell surface may thus constitute obligatory signals for transport.

We thank Drs. Bruce Granger and William Balch for helpful advice; Drs. Ira Mellman, Mary-Jane Gething, Joe Sambrook and the members of their laboratories for stimulating discussions; Drs. Carolyn Doyle and Mary-Jane Gething for providing us with expression vectors and with unpublished data; Drs. Peter Tattersall, Roland Baron, and Agnes Vignery for the use of equipment; Barbara Menzel for helpful technical assistance; Margaret Moench for artwork; Pam Ossorio for photography; Barbara Longobardi for secretarial help.

This work was supported by National Institutes of Health (NIH) Grant AI-18582 to A. Helenius and National Institute of Allergy and Infectious Disease Grant AI-08831 to R. G. Webster. C. Copeland received predoctoral fellowships from the National Science Foundation and from NIH training grant GM-07223.

Received for publication 25 June 1986, and in revised form 31 July 1986.

Note Added in Proof. The band coprecipitating with HA0 reacting with antibody A1 (Fig. 6 *A*) has been identified as BIP, based on lack of N-linked carbohydrate and reactivity with a monoclonal antibody specific for BIP (6).

References

1. Anderson, D. J., and G. Blobel. 1981. In vitro synthesis, glycosylation and membrane insertion of the four subunits of Torpedo acetylcholine receptor. *Proc. Natl. Acad. Sci. USA.* 78:5398–5602.

2. Anderson, R. G. W., and R. K. Pathak. 1985. Vesicles and cisternae in the trans Golgi apparatus of human fibroblasts are acidic compartments. *Cell.* 40:635–643.

3. Arce-Gomez, B., E. A. Jones, C. J. Barnstable, E. Solomon, and W. F. Bodmer. 1978. The genetic control of HLA-A and B antigens in somatic cell hybrids: requirement for beta-2-microglobulin. *Tissue Antigens.* 11:96–112.

4. Bächi, T., W. Gerhard, and J. W. Yewdell. 1985. Monoclonal antibodies detect different forms of influenza virus during viral penetration and biosynthesis. *J. Virol.* 55:307–313.

5. Balch, W. E., M. Elliott, and D. Keller. 1986. ATP-coupled transport of vesicular stomatitis virus G protein between the endoplasmic reticulum and the Golgi. *J. Biol. Chem.* In press.

6. Bole, D. G., L. M. Hendershot, and J. F. Kearney. 1986. Posttranslational association of immunoglobulin heavy chain binding protein with nascent heavy chains in nonsecreting and secreting hybridomas. *J. Cell Biol.* 102:1558–1566.

7. Brown, W. J., and M. G. Farquhar. 1984. The mannose-6-phosphate receptor for lysosomal enzymes is concentrated in *cis* Golgi cisternae. *Cell.* 36:295–307.

8. Campbell, A. M. 1984. Monoclonal Antibody Technology, Laboratory Techniques in Biochemistry and Molecular Biology. Vol. 13. R. H. Burdon, and P. M. van Knippenberg, editors. 389 pp.

9. Carlin, B. E., J. C. Lawrence, Jr., J. M. Lindstrom, and J. P. Merlie. 1986. An acetylcholine receptor precursor alpha subunit that binds alpha-bungarotoxin but not alpha-tubocurare. *Proc. Natl. Acad. Sci. USA.* 83:498–502.

10. Carlin, B. E., J. C. Lawrence, Jr., J. M. Lindstrom, and J. P. Merlie. 1986. Inhibition of acetylcholine receptor assembly by activity in primary cultures of embryonic rat muscle cells. *J. Biol. Chem.* 262:5180–5186.

11. Chamberlain, J. 1979. Fluorographic detection of radioactivity in polyacrylamide gels with the water-soluble fluor sodium salicylate. *Anal. Biochem.* 98:132–135.

12. Daniels, R. S., A. R. Douglas, J. J. Skehel, and D. C. Wiley. 1983. Analyses of the antigenicity of influenza haemagglutinin at the pH optimum for virus-mediated membrane fusion. *J. Gen. Virol.* 64:1657–1662.

13. Daniels, R. S., J. C. Downie, A. J. Hay, M. Knossow, J. J. Skehel, M. L. Wang, and D. Wiley. 1985. Fusion mutants of the influenza virus hemagglutinin glycoprotein. *Cell.* 431–439.

14. Doms, R. W., M.-J. Gething, J. Henneberry, J. White, and A. Helenius. 1986. Analysis of a variant influenza hemagglutinin that induces fusion at elevated pH. *J. Virol.* 57:603–613.

15. Doms, R. W., and A. Helenius. 1986. The quaternary structure of the influenza virus hemagglutinin after acid treatment. *J. Virol.* In press.

16. Doms, R. W., A. Helenius, and J. White. 1985. Membrane fusion activity of the influenza virus hemagglutinin. *J. Biol. Chem.* 260:2973–2981.

17. Doxsey, S., A. Helenius, and J. White. 1985. An efficient method for introducing macromolecules into living cells. *J. Cell Biol.* 101:19–27.

18. Doyle, C., J. Sambrook, and M.-J. Gething. 1986. Analysis of progressive deletions in the transmembrane and cytoplasmic domains of influenza hemagglutinin. *J. Cell Biol.* 103:1193–1204.

19. Dunphy, W. G., and J. S. Rothman. 1985. Compartmental organization of the Golgi stack. *Cell.* 42:13–21.

20. Garoff, H. 1986. Using recombinant DNA techniques to study protein targeting in the eukariotic cell. *Annu. Rev. Cell Biol.* 1:403–445.

21. Gerhard, W., J. Yewdell, M. E. Frankel, and R. Webster. 1981. Antigenic structure of influenza virus haemagglutinin defined by hybridoma antibodies. *Nature (Lond.).* 290:713–716.

22. Germain, R. N., D. M. Bentley, and H. Quill. 1985. Influence of allelic polymorphism on the assembly and surface expression of Class II MHC(Ia) molecules. *Cell.* 43:233–242.

23. Gething, M.-J., R. W. Doms, J. White, and A. Helenius. 1986. Studies on the mechanism of membrane fusion. Protein Engineering: Applications in Science, Medicine and Industry. M. Inouye and R. Sarma, editors. In press.

24. Gething, M.-J., R. W. Doms, D. York, and J. White. 1986. Studies on the mechanism of membrane fusion: site specific mutagenesis of the hemagglutinin of influenza virus. *J. Cell Biol.* 102:11–23.

25. Gething, M.-J., K. McCannon, and J. Sambrook. 1986. Expression of wildtype and mutant forms of influenza hemagglutinin: the role of folding in intracellular transport. *Cell.* In press.

26. Gething, M.-J., and J. Sambrook. 1982. Construction of influenza hemagglutinin genes that code for intracellular and secreted forms of the protein. *Nature (Lond.)* 300:598–603.

27. Jackson, D. C., and A. Nestorowicz. 1985. Antigenic determinants of influenza virus hemagglutinin XI. Conformational changes detected by monoclonal antibodies. *Virology.* 145:72–83.

28. Kondor-Koch, C., H. Riedel, K. Soderberg, and H. Garoff. 1982. Expression of the structural proteins of Semliki Forest virus from cloned cDNA microinjected into the nucleus of baby hamster kidney cells. *Proc. Natl. Acad. Sci. USA.* 79:4525–4529.

29. Kornfeld, R., and S. Kornfeld. 1985. Assembly of asparagine-linked oligosaccharides. *Annu. Rev. Biochem.* 54:631–664.

30. Kvist, S., K. Wiman, L. Claesson, P. Peterson, and B. Dobberstein. 1982. Membrane insertion and oligomeric assembly of HLA DR histocompatibility antigens. *Cell.* 29:61–69.

31. Laemmli, U. K. 1970. Cleavage of structural proteins during the assembly of the head of bacteriophage T4. *Nature (Lond.).* 227:680–685.

32. Lamb, R. A., and P. W. Choppin. 1983. The structure and replication of influenza virus. *Annu. Rev. Biochem.* 52:467–506.

33. Laver, W. G., and R. C. Valentine. 1969. Mophology of the isolated hemagglutinin and neuraminidase subunits of influenza virus. *Virology.* 38: 105–119.

34. Louvard, D., H. Reggio, and G. Warren. 1982. Antibodies to the Golgi complex and the rough endoplasmic reticulum. *J. Cell Biol.* 92:92–107.

35. Lusis, A. J., and K. Paigen. 1977. Mechanisms involved in the intracellular localization of mouse glucoronidase. *In* Isozymes: Current Topics in Biological and Medical Research. Vol. 2. M. C. Rattazzi, J. G. Scandalios, and G. S. Whitt, editors. Alan R. Liss Inc., New York. 63–106.

36. Machamer, C. E., and P. Cresswell. 1982. Biosynthesis and glycosylation of the invariant chain associated with HLA-DR antigen. *J. Immunol.* 129:2564–2569.

37. Matlin, K., and K. Simons. 1983. Reduced temperature prevents transfer of a membrane glycoprotein to the cell surface but does not prevent terminal glycosylation. *Cell.* 34:233–243.

38. Mellman, I. S., R. M. Steinman, J. C. Unkeless, and Z. A. Cohn. 1980. Selective iodination and polypeptide composition of pinocytic vesicles. *J. Cell Biol.* 86:712–722.

39. Merlie, J. P. 1984. Biogenesis of the acetylcholine receptor, a multisubunit integral membrane protein. *Cell.* 36:573–575.

40. Nestorowicz, A., G. Laver, and D. C. Jackson. 1985. Antigenic determinants of influenza virus hemagglutinin. *J. Gen. Virol.* 56:1687–1695.

41. Owen, M. J., A.-M. Kissonerghis, and H. F. Lodish. 1980. Biosynthesis of HLA-A and HLA-B antigens in vivo. *J. Biol. Chem.* 225:9678–9684.

42. Ploegh, H. L., L. E. Cannon, and J. L. Strominger. 1979. Cell-free translation of the mRNAs for the heavy and light chains of HLA-A and HLA-B antigens. *Proc. Natl. Acad. Sci. USA.* 76:2273–2277.

43. Peters, B. P., R. J. Hartle, R. F. Krzesicki, T. G. Kroll, F. Perini, J. E. Balun, I. J. Goldstein, and R. W. Ruddon. 1985. The biosynthesis, processing and secretion of laminin by human choriocarcinoma cells. *J. Biol. Chem.* 260:14732–14742.

44. Potter, T. A., R. A. Zeff, A.-M. Schmitt-Verholst, and T. V. Rajan. 1985. Molecular analysis of an EL-4 cell line that expresses H-2D^b but not H-2K^b or beta-2-microglobulin. *Proc. Natl. Acad. Sci. USA.* 82:2950–2954.

45. Rask, L., C. Valtersson, H. Anundi, S. Kvist, U. Eriksson, G. Dallner, and P. A. Peterson. 1983. Subcellular localization in normal and vitamin A-deficient rat liver of vitamin A serum transport proteins, albumin, ceruloplasmin and class I major histocompatibility antigens. *Exp. Cell Res.* 143:91–102.

46. Rodriguez-Boulan, E., K. T. Paskiet, P. J. I. Salas, and E. Bard. 1984. Intracellular transport of influenza virus hemagglutinin to the apical surface of Madin-Darby canine kidney cells. *J. Cell Biol.* 98:308–319.

47. Roth, M. G., C. Doyle, J. Sambrook, and M.-J. Gething. 1986. Heterologous transmembrane and cytoplasmic domains direct influenza hemagglutinin into the endocytic pathway. *J. Cell Biol.* 102:1271–1283.

48. Roth, M. G., M.-J. Gething, and J. Sambrook. 1986. Intracellular transport and membrane insertion of the influenza viral glycoproteins. *In* The Influenza Viruses. R. M. Krug, editor. Plenum Publishing Corp., New York. In press.

49. Skehel, J., P. Bayley, E. Brown, S. Martin, M. Waterfield, J. White, I. Wilson, and D. Wiley. 1982. Changes in the conformation of influenza virus hemagglutinin at the pH optimum of virus-mediated membrane fusion. *Proc. Natl. Acad. Sci. USA.* 79:968–972.

50. Ruigrok, R. W. H., N. G. Wrigley, L. J. Calder, S. Cusak, S. A. Wharton, E. B. Brown, and J. J. Skehel. 1986. Electron microscopy of the low pH structure of influenza virus hemagglutinin. *EMBO (Eur. Mol. Biol. Organ.) J.* 5:41–49.

51. Schmidt, M. F. G. 1982. Acylation of viral spike glycoproteins: a feature of enveloped RNA viruses. *Virology.* 116:327–338.

52. Schwartz, A. L., G. J. A. M. Strous, J. W. Slot, and H. J. Geuze. 1985. Immunoelectron microscopic localization of acidic intracellular compartments in hepatoma cells. *EMBO (Eur. Mol. Biol. Organ.) J.* 4:899–904.

53. Sege, K., L. Rask, and P. A. Peterson. 1981. Role of B2-microglobulin in the intracellular processing of HLA antigens. *Biochemistry.* 20:4523–4530.

54. Simons, K., A. Helenius, and H. Garoff. 1973. Solubilization of the membrane proteins from Semliki Forest Virus with Triton X-100. *J. Mol. Biol.* 80:119–133.

55. Springer, T. A., W. S. Thompson, L. J. Miller, F. C. Schmalstieg, and D. C. Anderson. 1984. Inherited deficiency of the Mac-1, LFA-1, p150,95 glycoprotein family and its molecular basis. *J. Exp. Med.* 160:1901–1918.

56. Steinman, R. M., I. Mellman, W. A. Muller, and Z. A. Cohn. 1983. Endocytosis and the recycling of plasma membrane. *J. Cell Biol.* 96:1–27.

57. Tarentino, A. L., R. B. Trimble, and F. Maley. 1978. Endo-beta-N-acetylglucosaminidase from Streptomyces plicatus. *Methods. Enzymol.* 50: 574–580.

58. Timm, B., C. Kondor-Koch, H. Lehrach, H. Riedel, J.-E. Edstrom, and H. Garoff. 1983. Expression of viral membrane proteins from cloned cDNA by microinjection into eukaryotic cell nuclei. *Methods Enzymol.* 96:496–511.

59. Towbin, H., T. Staehelin, and J. Gordon. 1979. Electrophoretic transfer of proteins from polyacrylamide gels to nitrocellulose sheets: procedure and some applications. *Proc. Natl. Acad. Sci. USA.* 76:4350–4354.

60. Ukkonen, P., V. Lewis, M. Marsh, A. Helenius, and I. Mellman. 1986. Transport of macrophage Fc receptors and Fc receptor-bound ligands to lysosomes. *J. Exp. Med.* 163:952–971.

61. Unkeless, J. C. 1979. Characterization of monoclonal antibody against mouse macrophage and lymphocyte Fc receptor. *J. Exp. Med.* 150:580–587.

62. Webster, R. G., L. E. Brown, and D. C. Jackson. 1983. Changes in the antigenicity of the hemagglutinin molecule of H3 influenza virus at acidic pH. *Virology.* 126:587–599.

63. Webster, R. G. and W. G. Laver. 1980. Determination of the number of nonoverlapping antigenic areas on Hong Kong (H3N2) influenza virus hemagglutinin with the selection of variants with potential epidemiological significance. *Virology.* 104:139–148.

64. White, J., M. Kielian, and A. Helenius. 1983. Membrane fusion proteins of enveloped animal viruses. *Quart. Rev. Biophys.* 16:151–195.

65. Wiley, D., I. A. Wilson, and J. J. Skehel. 1981. Structural identification of the antibody-binding sites of Hong Kong influenza haemagglutinin and their involvement in antigenic variation. *Nature (Lond.).* 289:373–378.

66. Wilson, I., J. Skehel, and D. Wiley. 1981. Structure of the hemagglutinin membrane glycoprotein of influenza virus at 3 Å resolution. *Nature (Lond.).* 289:366–373.

67. Yewdell, J. W., W. Gerhard, and T. Bächi. 1983. Monoclonal antihemagglutinin antibodies detect irreversible antigenic alterations that coincide with the acid activation of influenza virus A/PR/8/34-mediated hemolysis. *J. Virol.* 48:239–248.